Appl. Phys. B 52, 281–289 (1991)

Applied Physics B Photophysics and Laser Chemistry

Broadly Tunable Near-Infrared Six-Wave Mixing Processes in Potassium Vapor

Z. J. Jabbour, M. S. Malcuit, and J. Huennekens

Department of Physics, Lehigh University, Bethlehem, PA 18015, USA

Received 16 August 1990/Accepted 28 November 1990

Abstract. We report the observation of several six-wave mixing processes which result in broadly tunable coherent emission in the wavelength range 1.20–1.45 μm. These emissions are produced in potassium vapor which is simultaneously pumped by two pulsed dye lasers. One set of processes is produced when the frequency of the first laser is fixed to the potassium $4S \rightarrow 6S$ two-photon transition frequency, while the frequency of the second laser is tuned. The second set of processes is observed when both lasers are tuned, but with their sum frequency fixed to the $4S \rightarrow 6S$ two-photon transition. Peak output energies of ~10 nJ/pulse have been observed.

PACS: 42.65.Ky

Coherent emissions due to four- and six-wave mixing processes are commonly observed when alkali vapors are resonantly excited by high-power, pulsed lasers (see e.g. [1–7]). Coherent emission at a frequency ω can be described as arising from higher-order terms of the expansion of the induced polarization (vector component i) in powers of those electric fields present in the vapor [8]; i.e.,

$$\begin{aligned} P_i(\omega) = & \sum_j \chi_{ij}^{(1)}(\omega;\omega_p)E_j(\omega_p) \\ & + \sum_{j,k,l} \chi_{ijkl}^{(3)}(\omega;\omega_p,\omega_q,\omega_r)E_j(\omega_p)E_k(\omega_q)E_l(\omega_r) \\ & + \sum_{j,k,l,m,n} \chi_{ijklmn}^{(5)}(\omega;\omega_p,\omega_q,\omega_r,\omega_s,\omega_t) \\ & \times E_j(\omega_p)E_k(\omega_q)E_l(\omega_r)E_m(\omega_s)E_n(\omega_t) \\ & + \ldots, \end{aligned} \tag{1}$$

where the summations extend over the three Cartesian electric field components, and all allowed frequency combinations (see below) must be considered. In this expression, it is assumed that the medium is isotropic, so that only the odd order terms need be retained. Each of the susceptibility terms $\chi^{(n)}$ is, in general, a tensor of rank $n+1$. For the case when all electric fields are polarized parallel to each other and interact in an isotropic medium, $\chi^{(1)}$ is just the usual linear susceptibility $[P_i^{(1)}(\omega) = \chi^{(1)}E_i(\omega)]$, while $\chi^{(3)}$ and $\chi^{(5)}$ are given by (2) and (3), respectively [3, 8]:

$$\begin{aligned} & \chi^{(3)}(\omega;\omega_p,\omega_q,\omega_r) \\ & = \frac{KN}{\hbar^3} \sum_{a,b,c} \frac{\mu_{ga}\mu_{ab}\mu_{bc}\mu_{cg}}{(\omega_{ag} - \omega_p - i\gamma_{ag})\,(\omega_{bg} - (\omega_p + \omega_q) - i\gamma_{bg})} \\ & \quad \times \frac{1}{(\omega_{cg} - (\omega_p + \omega_q - \omega_r) - i\gamma_{cg})}; \end{aligned} \tag{2}$$

$$\begin{aligned} & \chi^{(5)}(\omega;\omega_p,\omega_q,\omega_r,\omega_s,\omega_t) \\ & = \frac{K'N}{\hbar^5} \sum_{a,b,c,d,e} \\ & \quad \times \frac{\mu_{ga}\mu_{ab}\mu_{bc}\mu_{cd}\mu_{de}\mu_{eg}}{(\omega_{ag} - \omega_p - i\gamma_{ag})\,(\omega_{bg} - (\omega_p + \omega_q) - i\gamma_{bg})} \\ & \quad \times \frac{1}{(\omega_{cg} - (\omega_p + \omega_q - \omega_r) - i\gamma_{cg})} \\ & \quad \times \frac{1}{(\omega_{dg} - (\omega_p + \omega_q - \omega_r - \omega_s) - i\gamma_{dg})} \\ & \quad \times \frac{1}{(\omega_{eg} - (\omega_p + \omega_q - \omega_r - \omega_s - \omega_t) - i\gamma_{eg})}. \end{aligned} \tag{3}$$

Here γ_{ag} is the decay rate of coherence between level a and the ground state g, $\omega_{ba} = (E_b - E_a)/\hbar$, μ_{ab} is the electric dipole matrix element coupling levels a and b, N is the atomic density, and K and K' are constants. In (2) and (3), the summations are over all atomic energy levels, and the equations are written to describe processes in

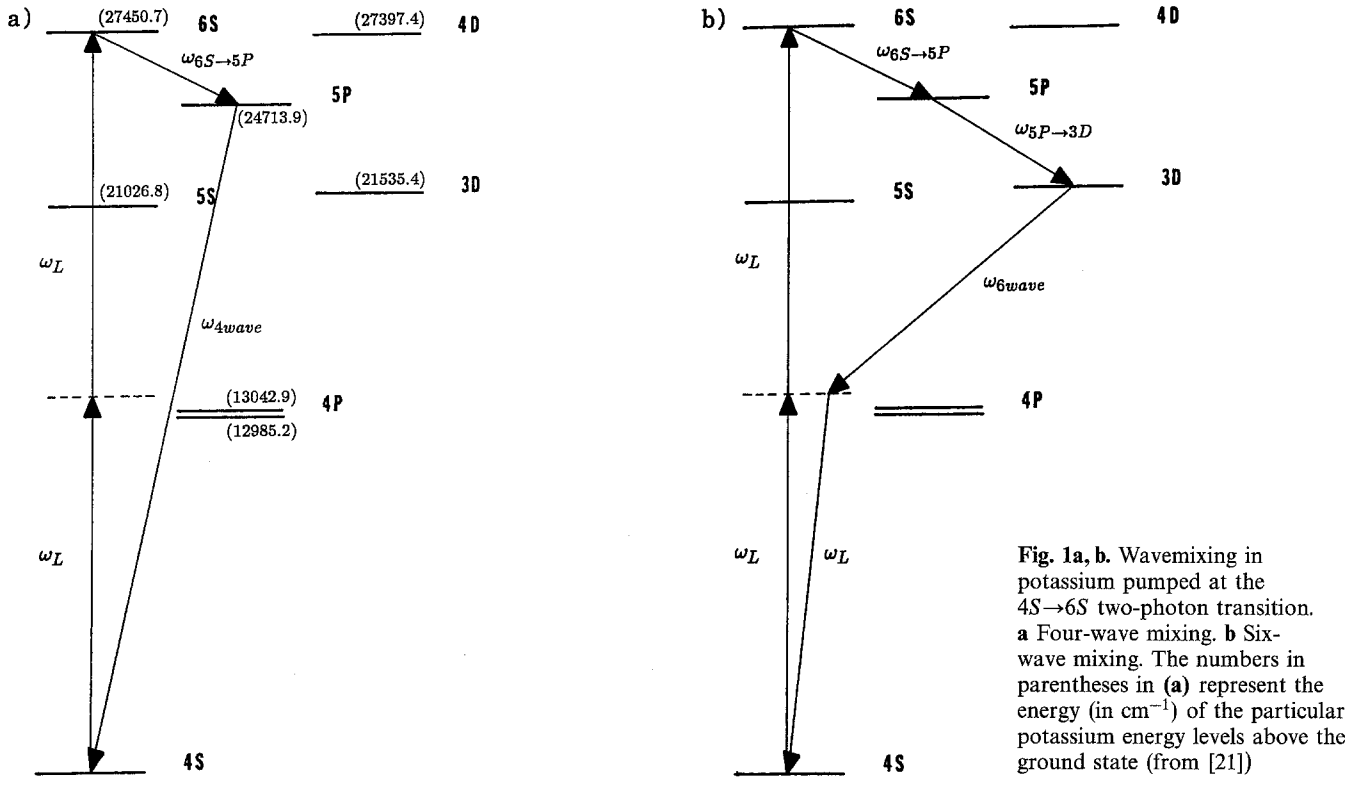

Fig. 1a, b. Wavemixing in potassium pumped at the $4S\rightarrow 6S$ two-photon transition. **a** Four-wave mixing. **b** Six-wave mixing. The numbers in parentheses in **(a)** represent the energy (in cm^{-1}) of the particular potassium energy levels above the ground state (from [21])

which two photons (ω_p and ω_q) are annihilated and the remaining photons are emitted. Examples of a four-wave process (resulting from a $\chi^{(3)}$ term) and a six-wave process ($\chi^{(5)}$) are shown in Fig. 1 for the case of potassium vapor pumped at the frequency of the $4S\rightarrow 6S$ two-photon transition [7, 9]. In these examples (as in most of the processes which have been observed in the alkalis), some of the **E** fields required to produce the wave-mixing signals are themselves produced by amplified spontaneous emission (ASE) or stimulated Raman scattering (SRS) in the vapor.

For the wave-mixing processes to be efficient, simple energy and momentum conservation expressions must be obeyed [8]. For example, in the case of the six-wave process shown in Fig. 1b, these expressions are:

$$2\omega_L = \omega_{6S\rightarrow 5P} + \omega_{5P\rightarrow 3D} + \omega_{6\,\mathrm{wave}} + \omega_L; \quad (4)$$

$$2\mathbf{k}_L = \mathbf{k}_{6S\rightarrow 5P} + \mathbf{k}_{5P\rightarrow 3D} + \mathbf{k}_{6\,\mathrm{wave}} + \mathbf{k}_L; \quad (5)$$

Here, $|\mathbf{k}| = \omega n(\omega)/c$ where $n(\omega)$ is the frequency dependent index of refraction, and ω_L is the pump laser frequency. We should note that in general, the ASE and SRS generated fields such as $\omega_{6S\rightarrow 5P}$ and $\omega_{5P\rightarrow 3D}$, may be slightly non-resonant and still satisfy the relevant equations. However, we will be considering cases of resonant two-photon excitations and low excited state populations, so that for our purposes these slight detunings are unimportant. The momentum conservation expression (5) is often called the phase-matching condition.

Generally, two types of phase-matching are possible [10, 11]. In a case such as that described by (4) and (5), the frequency of the six-wave mixing signal, $\omega_{6\,\mathrm{wave}}$, is fixed by the atomic transition and laser frequencies. Thus the wave vectors describing those fields which are produced in the vapor must adjust their directions to satisfy (5). In this "angle phase-matching", the generated waves typically propagate in cones centered on the pump laser direction. The small cone angles (typically a few milliradians) can be calculated from (4) and (5) if $n(\omega)$ is known. In the second type of phase-matching, the waves all propagate collinearly. In this case, the frequencies cannot be as tightly constrained as in (4); at least two of the photon frequencies must be free to vary:

$$2\omega_L = \omega_{6S\rightarrow 5P} + \omega_{5P\rightarrow 3D} + \omega_{\mathrm{axial}-1} + \omega_{\mathrm{axial}-2} \quad (6)$$

and

$$2|\mathbf{k}_L| = |\mathbf{k}_{6S\rightarrow 5P}| + |\mathbf{k}_{5P\rightarrow 3D}| + |\mathbf{k}_{\mathrm{axial}-1}| + |\mathbf{k}_{\mathrm{axial}-2}|. \quad (7)$$

Processes analogous to these were first predicted and observed in sodium vapor by Moore et al. [10], who called them "axially phase-matched" wave-mixing. Since then, other examples have been found in sodium [12, 13] and potassium [14, 15]. While most processes of this type are closely resonant with atomic dipole transitions, Luh et al. [12] showed that signal waves at fairly large detunings from atomic lines are also possible. Recently, Luh has calculated the wavelengths for many such processes in pure and mixed alkali vapors [16].

It has long been known that the output frequency of many of these wave-mixing processes can be made tunable by tuning the pump laser frequency [2, 17], or by varying the frequency dependence of the refractive index [12]. In the former case, it is found that near-resonant pumping of an allowed transition can produce strong tunable output due to SRS. The SRS wave can then couple to other waves in various wave-mixing processes and thus transfer its tunability to the generated waves. However,

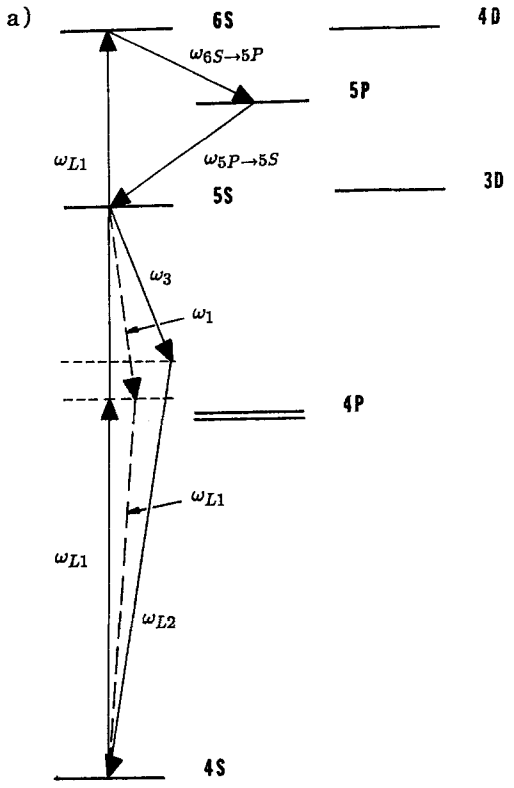

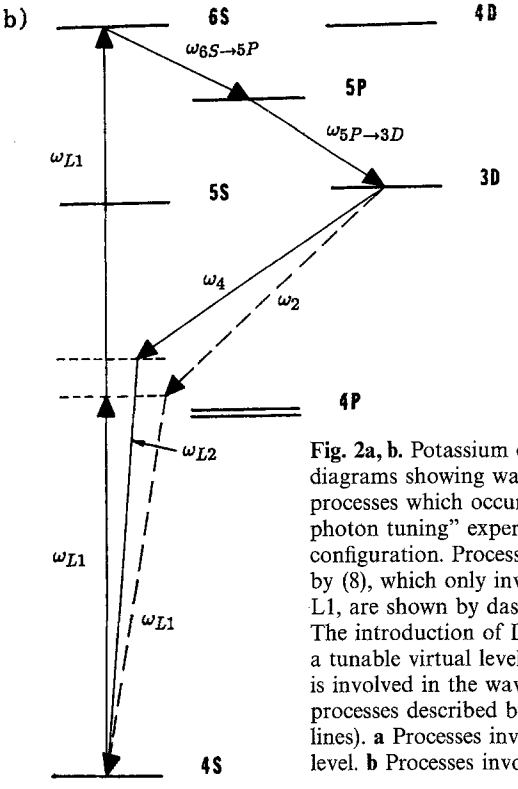

Fig. 2a, b. Potassium energy level diagrams showing wavemixing processes which occur in the "one-photon tuning" experimental configuration. Processes described by (8), which only involve laser L1, are shown by dashed lines. The introduction of L2 creates a tunable virtual level which is involved in the wavemixing processes described by (9) (solid lines). **a** Processes involving the 5*S* level. **b** Processes involving 3*D*

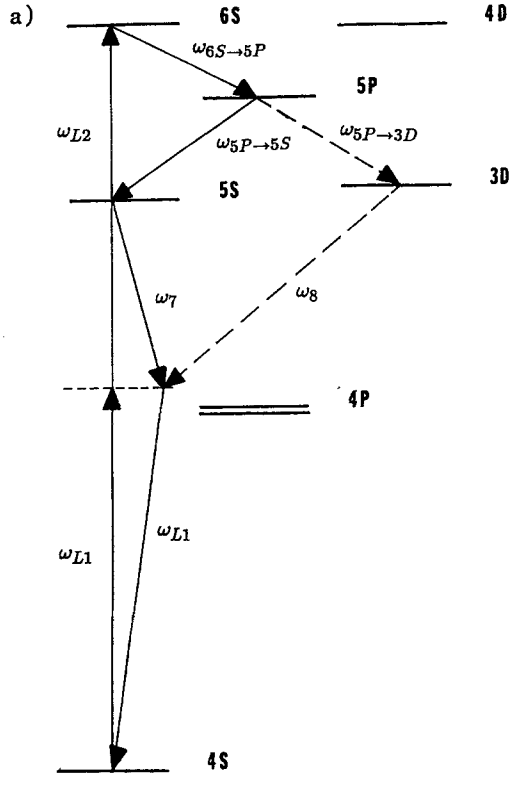

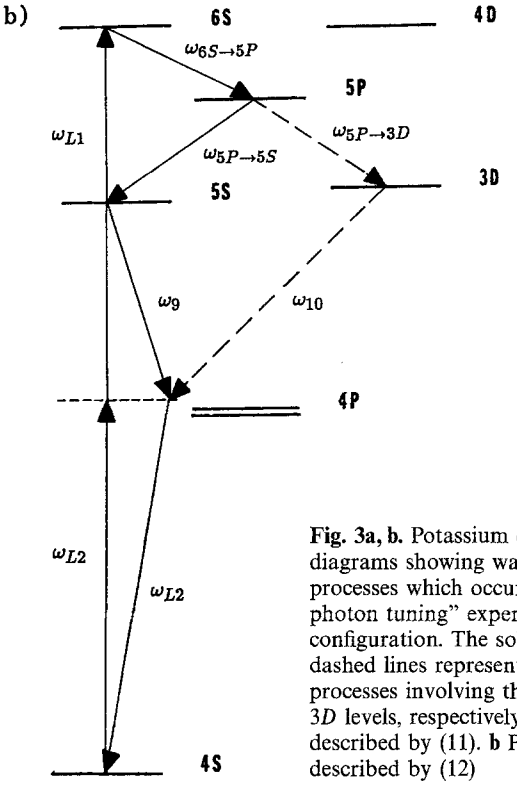

Fig. 3a, b. Potassium energy level diagrams showing wavemixing processes which occur in the "two-photon tuning" experimental configuration. The solid and dashed lines represent the processes involving the 5*S* and 3*D* levels, respectively. **a** Processes described by (11). **b** Processes described by (12)

such processes are resonantly enhanced, and therefore have a rather limited tuning range about the resonance (a few angstroms [2]). Broader tunability (~50 Å) has been observed for an axially phase-matched process by varying the composition of a sodium-potassium mixture [12]. However, the latter type of tuning is cumbersome, and difficult to control.

An alternative approach to tunability is through the use of more than one laser. In the present work, a second tunable laser was added to the scheme shown in Fig. 1. With the second tunable laser, several new wave mixing processes are allowed (Figs. 2 and 3). While the idea of using a second laser to tune the wave-mixing signal is certainly not new [18, 19], the results presented in this paper

demonstrate that the emissions from these wave mixing processes are very broadly tunable in the near-infrared where tunable light sources are not always readily available. In particular, the six-wave mixing signal shown in Fig. 1b is non-resonant by more than 1000 Å. With the addition of the second laser, as in Figs. 2 and 3, it is possible to tune the various emission frequencies, with fairly constant output power, over a range of several thousand angstroms. Thuse these processes represent a very inexpensive alternative to tunable near-infrared lasers (assuming that the necessary visible wavelength pulsed dye lasers are already available).

1. The Experiment

The experimental set-up is shown in Fig. 4. A 65 cm long linear stainless-steel heat-pipe oven [20] (with 25 cm heated region) containing pure potassium metal was used. It was operated at 420–425° C and with an argon buffer gas pressure of 10–12 Torr. Under these conditions, the heat-pipe oven was not operating in the heat-pipe mode; this allowed independent control of the temperature and buffer gas pressure.

A pulsed, frequency-doubled, Nd : YAG laser (pulse duration 6 ns) was used to pump two separate Littman type dye lasers: a Lumonics Hyperdye 300 (L1) and a homemade dye laser (L2). LDS 722 dye was used in both lasers. The tuning range of each laser was approximately 710–750 nm, with maximum pulse energies of 2 and 0.3 mJ (at ~ 728 nm) and linewidths of 0.1 and 2.6 Å for L1 and L2, respectively. The laser beams were combined using a beam splitter, propagated collinearly, and focused at the center of the heat pipe with a 30 cm focal length lens.

A long-pass, RG 850 filter was used to block the transmitted laser beams, and the infrared coherent emissions in the forward direction were focused onto the entrance slits of a 0.75 m monochromator (Spex model 1702). Calibrated neutral density filters were used to attenuate the infrared emissions which were detected using a liquid-nitrogen cooled, intrinsic germanium detector (Electro-Optics Systems model GLN-050/E70). Emissions in the visible range were detected using a photomultiplier (S-20 cathode). In either case, the signals were sent to a boxcar averager (Stanford Research System model SR250), and then to a chart recorder and computer for display and further analysis.

In one experiment, the frequency of laser L1 was set to the potassium $4S \rightarrow 6S$ two-photon transition frequency, while the frequency of laser L2 was varied. In this case, the second laser creates a tunable virtual level, and hence, generate two tunable six-wave mixing signals (Fig. 2). We refer to this technique as one-photon tuning. Another method, which we refer to as two-photon tuning, is shown schematically in Fig. 3. In this method, both lasers L1 and L2 were tuned such that their sum frequency matches the $4S \rightarrow 6S$ energy separation.

For both methods, the wavelength of the emission was analyzed with the lasers set to various frequencies. In order to clearly identify whether the observed signals were due to the effect of both lasers or either one alone, scans were taken with both lasers on, and with one or the other blocked. For all the scans, a barium hollow cathode lamp was used for wavelength calibration purposes.

2. Results and Discussion

2.1. One-Photon Tuning

When the potassium vapor is excited by tuning the frequency of laser L1 to half of the $4S \rightarrow 6S$ two-photon transition frequency, amplified spontaneous emissions (ASE), due to population inversions which exist as the atoms cascade through the atomic energy levels, are observed [7]. Also present in this case are two, angle phase-matched, six-wave mixing signals (ω_1 and ω_2) at wavelengths of 1.37 and 1.28 μm, respectively. These emissions are due to the coupling of two infrared and three laser photons according to the following mechanism:

$$2\omega_{L1} = \omega_{6S \rightarrow 5P} + \omega_{5P \rightarrow 5S,5P \rightarrow 3D} + \omega_{1,2} + \omega_{L1} . \quad (8)$$

When laser L2 is introduced, another coupling mechanism becomes possible. The generated infrared waves can couple to either ω_{L1} or ω_{L2} (Fig. 2) so that four six-

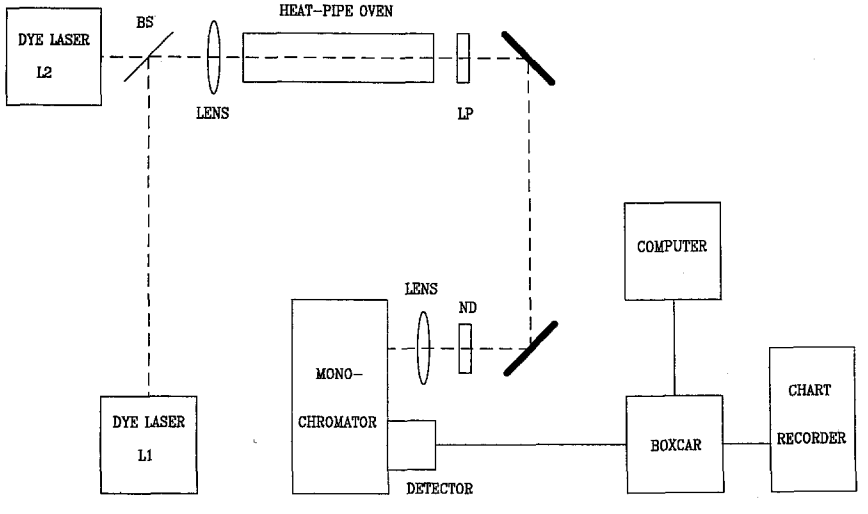

Fig. 4. Experimental set-up BS, LP, and ND represent beam splitter, long-pass filter, and neutral density filter, respectively

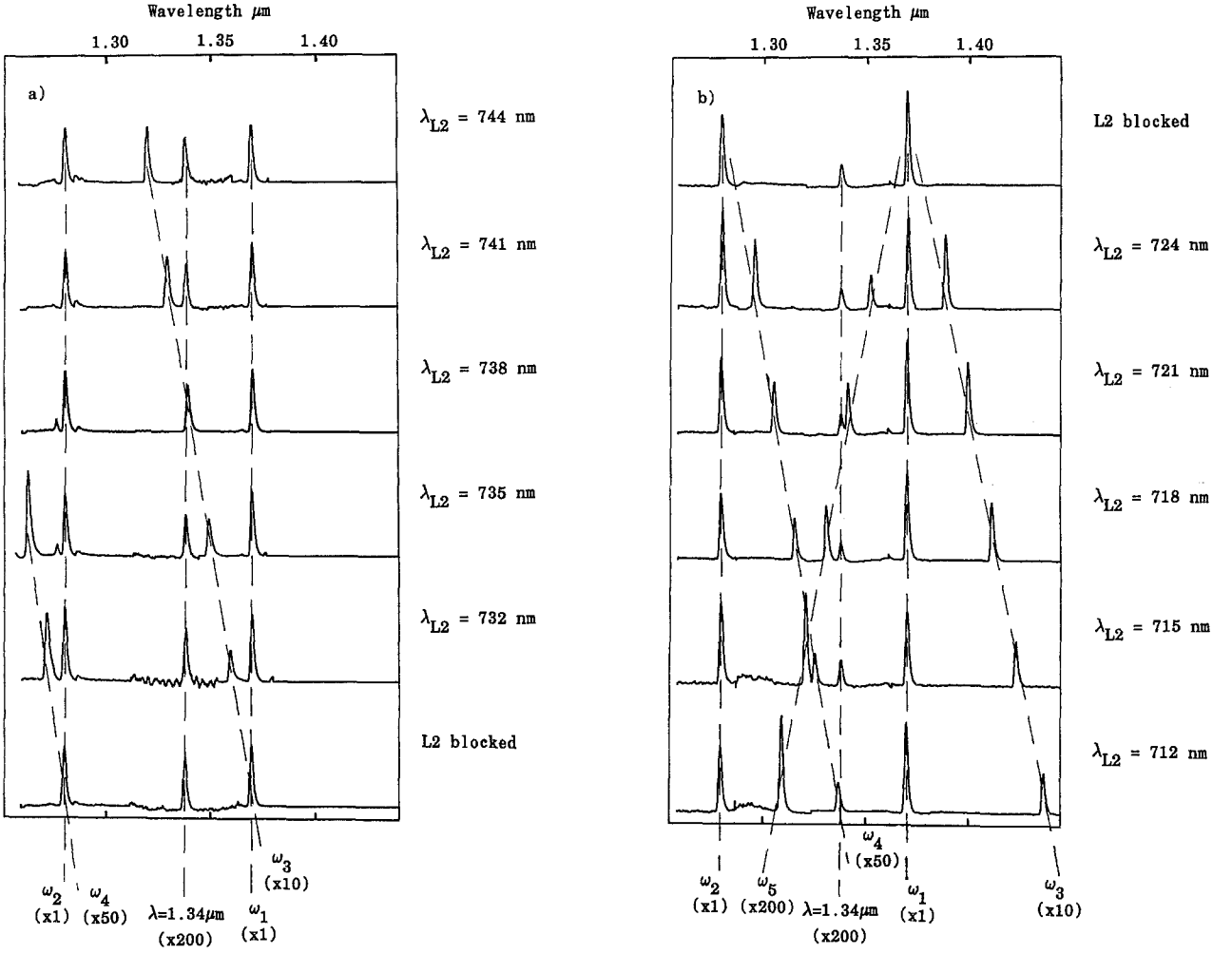

Fig. 5a, b. Emission scans recorded in the one-photon tuning experiment showing the fixed wavelength ω_1, ω_2, and $\lambda = 1.34\,\mu m$ lines, and the tunable ω_3, ω_4, and ω_5 lines. **a** $\lambda_{L2} > \lambda_{L1} = 728.4\,nm$. **b** $\lambda_{L2} < \lambda_{L1} = 728.4\,nm$. Dashed lines are added to guide the eye. Neutral density filters were inserted and removed during the scans in order to make large scale changes. The data shown in **a** were taken on a different day than those of **b**. Due to slight differences which occur in the heat-pipe oven operating conditions from day to day, intensities in **a** cannot be directly compared to those in **b**

wave mixing signals are observed. Two of these signals (ω_1 and ω_2) are due to coupling with ω_{L1} given by (8) while the other two (ω_3 and ω_4) are due to coupling with ω_{L2}:

$$2\omega_{L1} = \omega_{6S\to 5P} + \omega_{5P\to 5S,5P\to 3D} + \omega_{3,4} + \omega_{L2}\,. \tag{9}$$

When a tunable source is used for L2, ω_3 and ω_4 become tunable, as can be seen from (9). We have experimentally demonstrated the tunability of the six-wave mixing signals described by (9). This tunability is shown in the emission scans of Fig. 5, where the wavelength of laser L2 was tuned from 712 to 744 nm, causing the wavelengths of the six-wave mixing signals ω_3 and ω_4 to vary from 1.43 to 1.32 μm and from 1.34 to 1.21 μm, respectively.

Besides the lines predicted by (9), another line (ω_5), tunable from 1.37 to 1.31 μm, was also observed (Fig. 5). This line can be attributed to a six-wave mixing process, shown in Fig. 6, involving the coupling of two ASE-generated infrared photons with two L1 and one L2 photons such that:

$$\omega_{L1} + \omega_{L2} = \omega_{6S\to 5P} + \omega_{5P\to 5S} + \omega_5 + \omega_{L1}\,. \tag{10}$$

The ω_5 line is symmetric with ω_3 about the fixed frequency 1.37 μm line and tunes with ω_{L2}, but in the opposite direction of ω_3. This is because ω_{L2} appears on the left-hand side of (10) and on the right-hand side of (9). The analogous process (ω_6), involving the $3D$ level (instead of the $5S$), is not visible in Fig. 5 since it is much weaker and occurs in the region of strong ASE lines near 1.24–1.25 μm. However, we scanned with higher sensitivity and were able to confirm that the ω_6 process was present and tunable on the blue side of the 1.28 μm line.

From (1, 2, 3) and the wave equations [8], it can be shown that the intensity of a particular six-wave mixing signal depends on the amplitudes of the fields involved in its generation, and on $\chi^{(5)}$. From (3), we see that $\chi^{(5)}$ is greatly increased by resonant enhancement. This effect is clearly observed in Fig. 5. When laser L2 is tuned farther from the potassium $4S\to 4P$ transition frequency, the ω_3 and ω_4 signals also move farther from the $5S\to 4P$ and $3D\to 4P$ resonance lines, respectively, and their intensities gradually decrease. Under the same conditions, the ω_5 line becomes stronger since it moves closer to the $5S\to 4P$ resonance. The resonant enhancement also par-

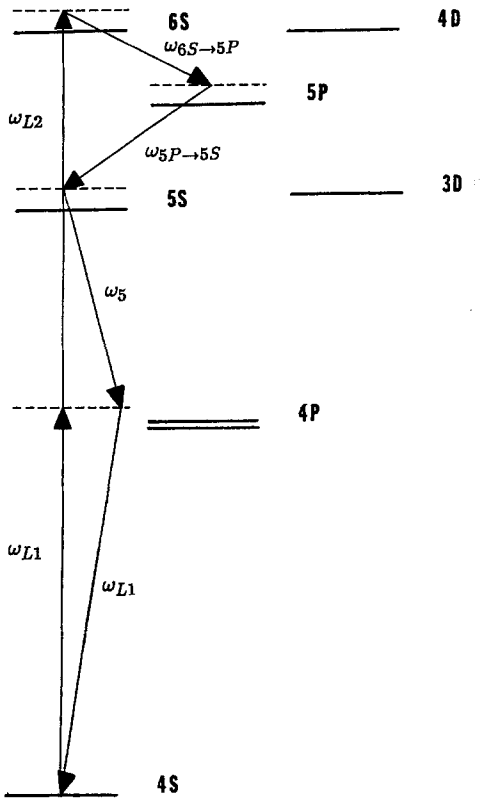

Fig. 6. Six-wave mixing process described by (10) which produces the tunable output ω_5

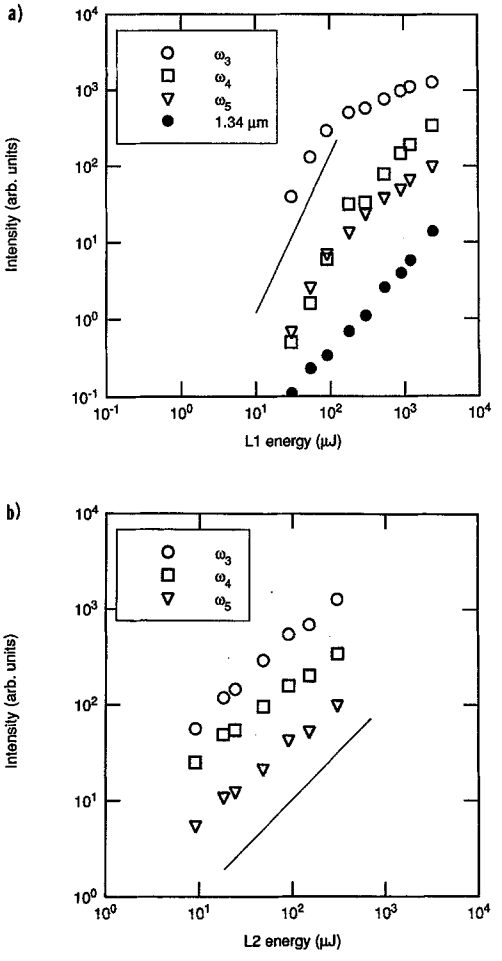

Fig. 7a, b. Dependence of the tunable wavemixing signals ω_3, ω_4, and ω_5 on **a** laser L1 energy, and **b** laser L2 energy, when λ_{L2} = 721 nm. The solid lines shown in **a** and **b** have slopes of 2 and 1, respectively. The L1 energy dependence of the fixed frequency 1.34 μm line is also shown in **a**

tially explains the absence of the $\omega_{5,6}$ lines in Fig. 5a, since in this case as L2 tunes to longer wavelength, ω_5 and ω_6 move farther from the $5S\rightarrow 4P$ and $3D\rightarrow 4P$ resonances, while ω_3 and ω_4 move closer to these resonances.

The dependence of the signal $(\omega_3, \omega_4, \omega_5)$ intensities on L1 and L2 laser energies for L2 tuned to $\lambda = 721$ nm is shown in Figs. 7a and b. It can be seen that our highest available laser powers place us in the saturation limit with respect to L1, but in the expected linear regime with respect to L2. At lower values of L1 energy, these wavemixing signals are seen to scale approximately quadratically with L1 energy, as we expect from (9) and (10). When L2 was tuned to 724 nm, a maximum output energy of 10 nJ was measured for the six-wave mixing signal at ω_3. We expect that this could be significantly increased if a more powerful, narrowband second laser was used, if further improvements were made in the beam overlap and focusing, and if the heat-pipe parameters were optimized. The 10 nJ measured for the ω_3 output represents a conversion efficiency of 0.0033% with respect to the L2 pulse energy. Processes ω_4 and ω_5 have conversion efficiencies which are lower than that of ω_3 by factors of 5 and 45, respectively.

2.2. *Two-Photon Tuning*

When the frequencies of both lasers L1 and L2 are varied such that their sum matches the $4S\rightarrow 6S$ two-photon transition frequency (Fig. 3), the six-wave mixing signal frequencies, $\omega_7 - \omega_{10}$, depend on whether the process couples to two L1 and one L2 photon, or vice-versa; i.e.,

$$\omega_{L1} + \omega_{L2} = \omega_{6S\rightarrow 5P} + \omega_{5P\rightarrow 5S,5P\rightarrow 3D} + \omega_{7,8} + \omega_{L1} \quad (11)$$

or

$$\omega_{L1} + \omega_{L2} = \omega_{6S\rightarrow 5P} + \omega_{5P\rightarrow 5S,5P\rightarrow 3D} + \omega_{9,10} + \omega_{L2}\,. \quad (12)$$

Again this coupling results in four six-wave mixing lines, $\omega_7 - \omega_{10}$, due to the two possible cascade channels through the $5S$ and $3D$ levels. Note also, that the process outlined in (11) is the same as (10), except that in (11) both ω_{L1} and ω_{L2} are varied with $\omega_{L1} + \omega_{L2} = \omega_{6S\rightarrow 4S}$, while in (10), ω_{L1} is fixed according to $2\omega_{L1} = \omega_{6S\rightarrow 4S}$.

In our experimental work, the $\omega_7 - \omega_{10}$ lines shown in Fig. 8 are much weaker than the corresponding lines of the one-photon tuning process. Presumably, these lines are weaker since in this case the $6S$ state is populated by a two-photon transition involving one photon from each laser. Laser L2 is not only weaker than L1, but also spectrally much broader. Thus the $6S$ state population is small compared to the one-photon tuning case, which in turn reduces the intensities of the ASE fields $\omega_{6S\rightarrow 5P}$, $\omega_{5P\rightarrow 5S}$, and $\omega_{5P\rightarrow 3D}$.

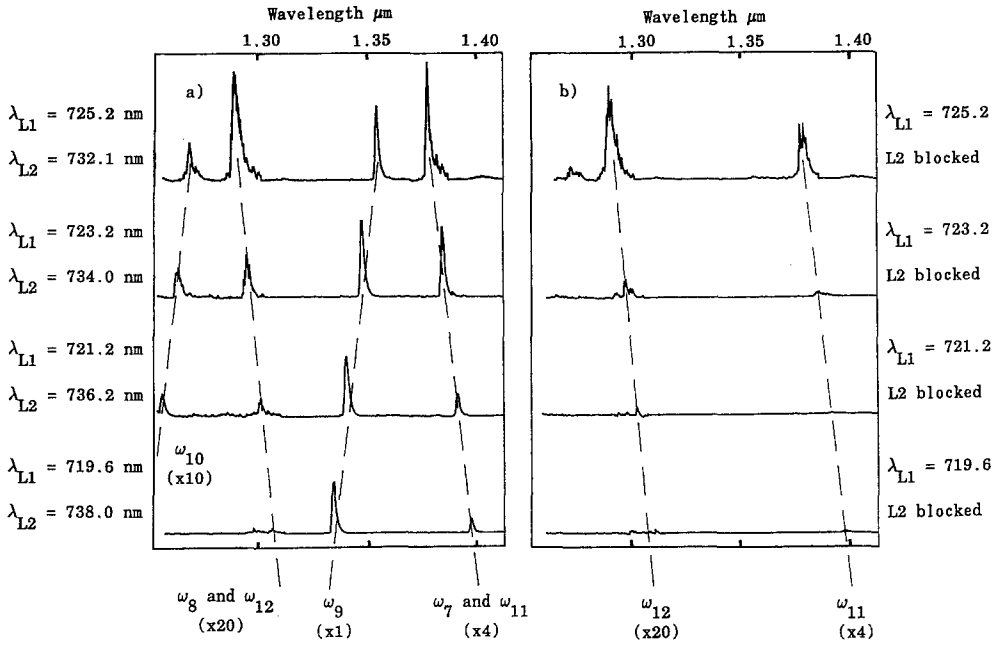

Fig. 8a, b. Emission scans recorded in the two-photon tuning experiment showing the tunable $\omega_7 - \omega_{12}$ lines described by (11–14). **a** $\omega_{L1} + \omega_{L2} = \omega_{6S\to 4S}$. **b** Same as **a**, but laser L2 blocked. Part **b** shows the contribution to the signals in **a** labeled "ω_8 and ω_{12}" and "ω_7 and ω_{11}" from the SHR-initiated processes ω_{11} and ω_{12}. Dashed lines are added to guide the eye

With L1 on, but L2 blocked, we see from Fig. 8 that two of the six-wave mixing signals are still present, but weaker. The generation of these signals in this case is initiated by a stimulated-hyper-Raman (SHR) process illustrated in Fig. 9 and described by:

$$2\omega_{L1} = \omega_{SHR} + \omega_{5P\to 5S,5P\to 3D} + \omega_{11,12} + \omega_{L1} \tag{13}$$

with

$$\omega_{SHR} = 2\omega_{L1} - \omega_{5P\to 4S}\,. \tag{14}$$

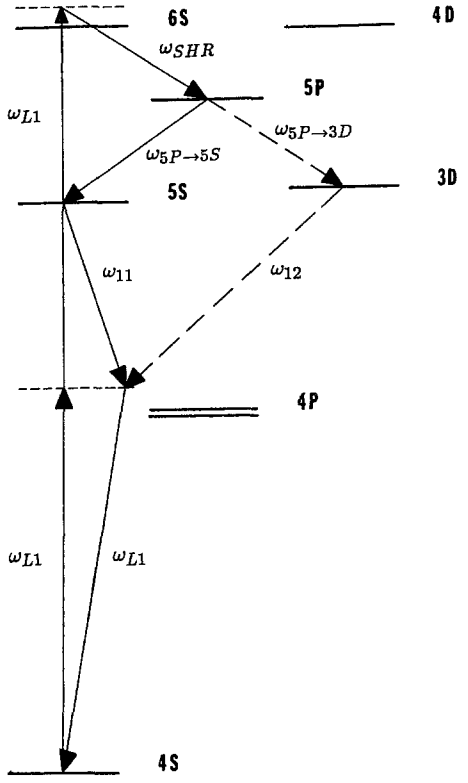

Fig. 9. Stimulated-hyper-Raman initiated six-wave mixing process $(\omega_{11}, \omega_{12})$ described by (13) and (14)

The emission seen ar $\omega_7(\omega_8)$ in Fig. 8a is therefore a combination of the $\omega_7(\omega_8)$ process from (11) and the $\omega_{11}(\omega_{12})$ process from (13). The stimulated hyper-Raman emission at ω_{SHR} was not observed since it lies outside the useful range of our detector.

Similar SHR processing involving the L2 laser must also occur at the same frequencies as ω_9 and ω_{10}. These were not observed experimentally; a fact which we attribute to the weakness of L2 relative to L1.

The dependence of the ω_7 and ω_9 signals on laser energies when $\lambda_{L1} = 723.2\,\text{nm}$ and $\lambda_{L2} = 734.0\,\text{nm}$ is shown in Fig. 10a, b. The approximate quadratic dependence of ω_9 and linear dependence of ω_7 on L2 energy in the high energy limit (Fig. 10b) is as expected from (11) and (12). At lower L2 energy, the "ω_7 and ω_{11}" signal is dominated by the ω_{11} process (13, 14) and is therefore independent of L2 energy. From (11) and (12) we expect ω_7 to scale quadratically, and ω_9 to scale linearly, with L1 energy. While the former is approximately as observed below the saturation limit (Fig. 10a), the latter clearly is not. At present, we have no explanation for the observed very strong dependence of ω_9 on L1 energy.

2.3. *Other Forward Emissions*

Other coherent emissions were observed at 1.172, 1.244, 1.246, 1.253, and 1.338 μm when $2\omega_{L1} = \omega_{6S\to 4S}$. None of these lines depended on the presence of L2. The 1.244 and 1.253 μm emissions correspond to amplified spontaneous emission and wave mixing on the $5S\to 4P$ transitions. The 1.172 and 1.246 μm lines are attributed to axially phase-matched six-wave mixing processes involving the $3D$ and $5S$ levels, respectively. The processes corresponding to the $5S$ level are shown in Fig. 11. A theoretical calculation of the axial emission wavelength must satisfy (6) and (7) with $k = n(\omega)\omega/c$ and the frequency dependent refractive index given by [12]:

$$n - 1 \approx \frac{2\pi e^2}{m} \sum_{a,b} \frac{N_a f_{ab}}{\omega_{ab}^2 - \omega^2}\,, \tag{15}$$

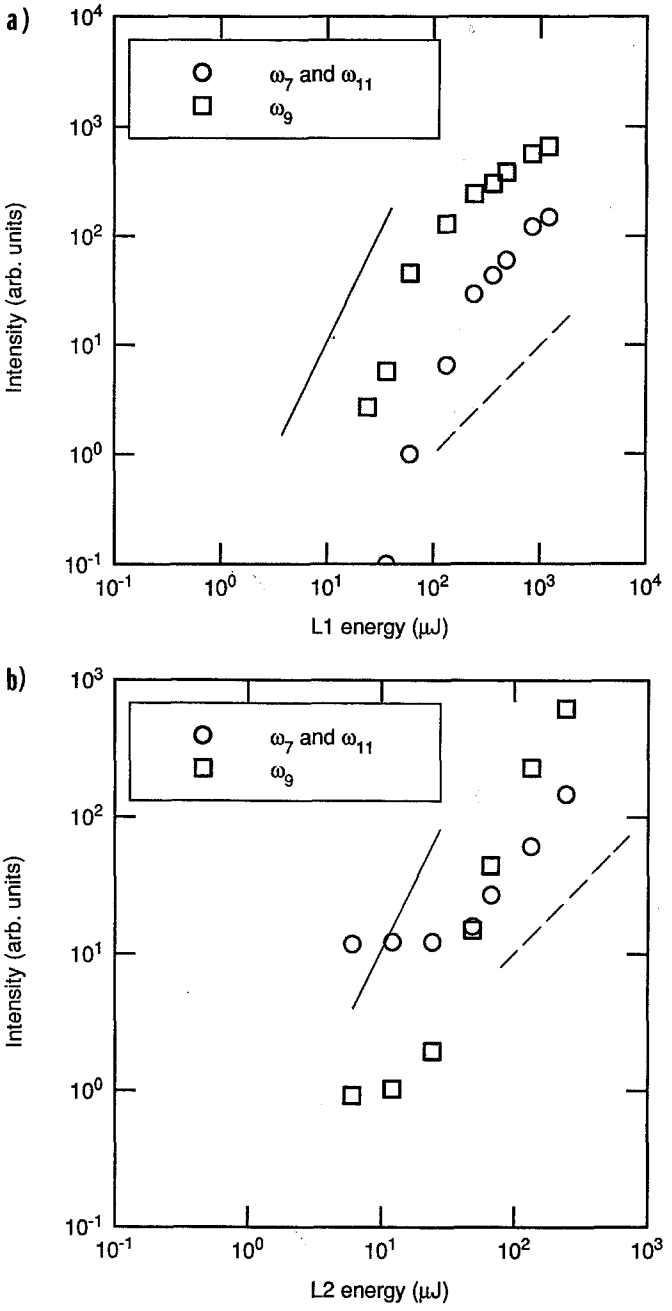

Fig. 10a, b. Dependence of the two-photon tuning wavemixing signals ω_9, and ω_7 plus ω_{11} on **a** laser L1 energy, and **b** laser L2 energy. $\lambda_{L1} = 723.2$ nm. $\lambda_{L2} = 734.0$ nm. The solid and dashed straight lines in the figures have slopes of 2 and 1, respectively

where N_a is the atom density in level a, and f_{ab} is the oscillator strength for the transition from level a to level b. These calculations predict the observed lines at 1.172 and 1.246 μm. Similar processes have been observed in sodium vapor by Moore et al. [10] and Wunderlich et al. [13].

The 1.338 μm emission, which is easily seen in Fig. 5, is still a mystery to us. It depends on L1 alone and is only present when $2\omega_{L1} = \omega_{6S\to 4S}$. The wavelength of this emission agrees with that of the potassium $6P\to 3D$ transition within our measuring accuracy, and it is likely that this emission is produced by one or more resonantly enhanced wavemixing processes which can be constructed

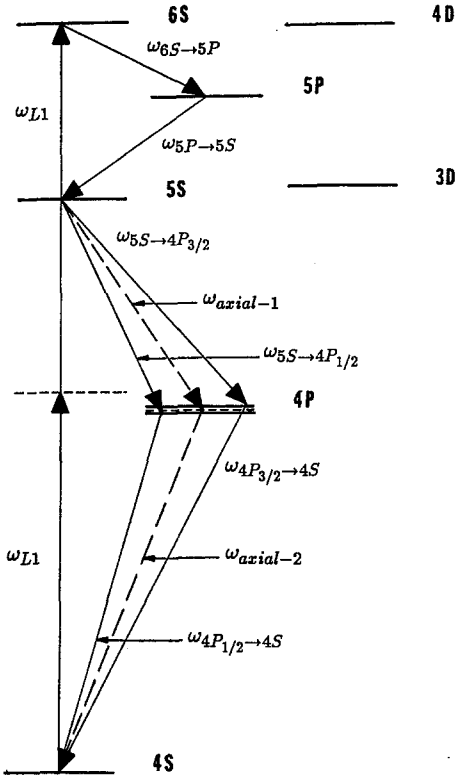

Fig. 11. Axial and angle phase-matched six-wave mixing processes, involving the 5S state, which result in coherent emissions in the 1.24–1.26 μm region

from the many available fields. As seen in Fig. 7a, the 1.338 μm signal depends linearly on the L1 energy over the range studied.

Other coherent emissions were also observed in the visible and near-UV when we replaced the germanium detector by a photomultiplier. These signals can all be attributed to four- and six-wave mixing processes involving two laser photons and the infrared photons generated by the six-wave mixing processes discussed above. Some of these emissions also occur at transition frequencies involving levels above the pumped 6S state.

3. Conclusions

By using two independently tunable dye lasers, we have demonstrated the possibility of generating broadly tunable coherent near-infrared radiation using six-wave mixing processes in potassium vapor. Using the "one-photon tuning" scheme described in Sect. 2.1, a tuning range of 1.20 to 1.45 μm, with nanojoule energies, was achieved. We believe that significantly higher output energies can be reached if stronger pump lasers are used. In addition, a wider tuning range could also be obtained using additional dyes.

A "two-photon tuning" scheme (Sect. 2.2) was also investigated. This technique provides an alternative method of generating tunable near-IR emission which may be of value in cases where the dyes necessary for "one-photon tuning" are unavailable. However, with the pump lasers available to us, the one-photon tuning is to be preferred

since it offers a greater tuning range, higher output power, and a less cumbersome tuning procedure.

Acknowledgement. This work was supported by the Army Research Office under grant DAAL03-89-K-0171.

References

1. O.J. Lumpkin, Jr.: IEEE J. QE-**4**, 226 (1968)
2. W. Hartig: Appl. Phys. **15**, 427 (1978)
3. P.-L. Zhang, Y.-C. Wang, A.L. Schawlow: J. Opt. Soc. Am. B **1**, 9 (1984)
4. J. Krasinski, D.J. Gauthier, M.S. Malcuit, R.W. Boyd: Opt. Commun. **54**, 241 (1985)
5. S.M. Hamadani, J.A.D. Stockdale, R.N. Compton, M.S. Pindzola: Phys. Rev. A **34**, 1938 (1986)
6. Z.G. Wang, H. Schmidt, B. Wellegehausen: Appl. Phys. B **44**, 41 (1987)
7. B.K. Clark, M. Masters, J. Huennekens: Appl. Phys. B **47**, 159 (1988)
8. Y.R. Shen: *The Principles of Nonlinear Optics* (Wiley, New York 1984)
9. S. Barak, M. Rokni, S. Yatsiv: IEEE J. QE-**5**, 448 (1969)
10. M.A. Moore, W.R. Garrett, M.G. Payne: Phys. Rev. A **39**, 3692 (1989)
11. M.A. Moore: Ph.D. dissertation, University of Tennessee (unpublished)
12. W.T. Luh, Y. Li, J. Huennekens: Appl. Phys. B **49**, 349 (1989)
13. R.K. Wunderlich, W.R. Garrett, R.C. Hart, M.A. Moore, M.G. Payne: Phys. Rev. A **41**, 6345 (1990)
14. B.K. Clark: Private communication
15. R.N. Compton: Private communication
16. W.T. Luh: Chin. J. Phys. **28**, 139 (1990)
17. D. Cotter, D.C. Hanna, W.H.W. Tuttlebee, M.A. Yuratich: Opt. Commun. **22**, 190 (1977)
18. P.P. Sorokin, J.J. Wynne, J.R. Lankard: Appl. Phys. Lett. **22**, 342 (1973)
19. D.J. Jackson, J.J. Wynne: Appl. Phys. B **28**, 238 (1982)
20. C.R. Vidal, J. Cooper: Appl. Phys. **40**, 3370 (1969)
21. W.L. Wiese, M.W. Smith, B.M. Miles: *Atomic Transition Probabilities*, Vol. II, NSRDS-NBS 22 (1969)